Published in final edited form as:
Nat Struct Biol. 2002 January ; 9(1): 27–31. doi:10.1038/nsb737.

The crystal structure of spermidine synthase with a multisubstrate adduct inhibitor

Sergey Korolev[1], **Yoshihiko Ikeguchi**[2], **Tatiana Skarina**[3], **Steven Beasley**[3], **Cheryl Arrowsmith**[3], **Aled Edwards**[3,4], **Andrzej Joachimiak**[1], **Anthony E. Pegg**[2], and **Alexei Savchenko**[3]

[1]Biosciences Division and Structural Biology Center, Argonne National Laboratory, 9700 South Cass Ave., Bldg. 202, Argonne, Illinois 60439, USA.

[2]Department of Cellular and Molecular Physiology, Pennsylvania State University College of Medicine, The Milton S. Hershey Medical Center, P.O. Box 850, 500 University Drive, Hershey, Pennsylvania 17033, USA.

[3]Banting and Best Department of Medical Research, 112 College St., Toronto, Ontario, M5G 1L6, Canada.

[4]Clinical Genomics Centre/Proteomics, University Health Network, 101 College St., Toronto, Ontario, M5G 1L7, Canada.

Abstract

Polyamines are essential in all branches of life. Spermidine synthase (putrescine aminopropyltransferase, PAPT) catalyzes the biosynthesis of spermidine, a ubiquitous polyamine. The crystal structure of the PAPT from *Thermotoga maritima* (TmPAPT) has been solved to 1.5 Å resolution in the presence and absence of AdoDATO (*S*-adenosyl-1,8-diamino-3-thiooctane), a compound containing both substrate and product moieties. This, the first structure of an aminopropyltransferase, reveals deep cavities for binding substrate and cofactor, and a loop that envelops the active site. The AdoDATO binding site is lined with residues conserved in PAPT enzymes from bacteria to humans, suggesting a universal catalytic mechanism. Other conserved residues act sterically to provide a structural basis for polyamine specificity. The enzyme is tetrameric; each monomer consists of a C-terminal domain with a Rossmann-like fold and an N-terminal β-stranded domain. The tetramer is assembled using a novel barrel-type oligomerization motif.

The nearly ubiquitous polyamines (putrescine, spermidine and spermine) are polycationic mediators of cell proliferation and differentiation[1] whose functions likely provide both stability and neutralization for nucleic acids. The abundance of polyamines is tightly regulated through biosynthesis, degradation, uptake and efflux[2]. The biosynthesis of polyamines is carried out by three highly conserved polyamine biosynthetic enzymes (Fig. 1): ornithine decarboxylase, putrescine amino-propyltransferase (PAPT) and spermidine aminopropyltransferase (SAPT). The strong correlation of polyamine synthesis with cell growth renders these aminopropyl transferases (APTs) attractive targets for the development of antiproliferative therapeutics. The APTs are known to be inhibited by their common nucleoside product, as well as other nucleoside analogs. Most inhibitors, such as the nucleoside-polyamine adduct

Correspondence should be addressed to A.J. andrzejj@anl.gov or A.E. aled.edwards@utoronto.ca or A.E.P. aepl@psu.edu.

adenosylspermidine[3], target the active site of the enzyme. The combined substrate-product analog, *S*-adenosyl-1,8-diamino-3-thiooctane (AdoDATO)[4], is also a potent inhibitor of PAPT.

The catalytic mechanism of polyamine biosynthesis is unclear, partly because there is no detailed structural information for this class of enzymes. To provide structural insights into the mechanism of spermidine synthesis, the crystal structure of PAPT from *Thermotoga maritima* (TmPAPT) was determined at high resolution in ligand-free and AdoDATO-bound states. These structures provide insight into the function of the enzyme and its potential mechanism of action. The identification of conserved active site residues should enable accurate models of the mammalian enzymes.

The PAPT fold

The structure of TmPAPT was solved using multiwavelength anomalous diffraction (MAD) from selenomethionine (SeMet)-containing crystals. The TmPAPT monomer consists of two domains: an N-terminal domain, composed of six β-strands, and a Rossmann-like C-terminal domain (Fig. 2). The larger C-terminal catalytic core domain (residues 75–296) consists of a seven-stranded β-sheet with a strand order of 9↑, 8↑, 7↑, 10↑, 11↑, 13↓, 12↑ flanked by nine α-helices. This domain resembles a topology observed in a number of nucleotide and dinucleotide-binding enzymes[5], and in *S*-adenosyl-L-methionine (AdoMet)-dependent methyltransferases[6] (MTases). A search for structurally similar proteins using DALI[7] revealed catechol O-Mtase[8], with a Z-score of 12.3 and a root mean square (r.m.s.) deviation of 3.1 Å for Cα atoms of 165 equivalent residues; glycine N-Mtase[9] (Z-score = 12.2 and r.m.s. deviation = 3.7 Å for 157 residues) and adenine-N6-DNA-Mtase[10] (Z-score = 12.3 and r.m.s. deviation = 3.4 Å for 158 residues). A PAPT family signature V-(LA)-(LIV)(2)-G-G-G-X-G-X(2)-(LIV)-X-E (where X is any amino acid) has been previously defined (PROSITE entry PS01330)[11]; this motif is located at the end of β7 and corresponds structurally to motif I in Mtases[12]. In these MTases, the catalytic residues are located in the P-loop (motif IV). The corresponding loop in TmPAPT consists of residues 171–180 (loop β10–αE), which are disordered in three of the four molecules in the asymmetric unit of the crystal. The first two strands of the N-terminal domain form a hairpin, followed by a four-stranded β-sheet attached to the top of the core domain that forms part of the active site (see below). Apart from the unstructured loop and a few N- and C-terminal residues, all four subunits have an identical structure, with an overall r.m.s. deviation between coordinates of all Cα atoms in the range of 0.25–0.3 Å.

Oligomeric structure

The PAPT orthologs from *Escherichia coli*, rat, bovine and human sources are thought to be dimers[3]. The TmPAPT enzyme is a tetramer in the crystal (Fig. 2*b*) and in solution (confirmed by size exclusion chromatography; data not shown), suggesting that the tetramer represents the functional oligomeric form of TmPAPT. The tetramer is maintained by a tight β-barrel with a strong hydrophobic core formed by the four N-terminal β-hairpins. Tetramerization possibly underlies its thermostability because oligomerization is known to increase protein stability by reducing the solvent-accessible surface[13].

PAPT enzymatic activity and polyamine synthesis

Because all known SAPTs and PAPTs are similar in sequence, characterizing the *Thermotoga maritima* enzyme was important. TmPAPT was unequivocally identified as a spermidine synthase because spermidine and MTA (5′-methylthioadenosine) were formed when it was incubated with putrescine and dcAdoMet (decarboxylated *S*-adenosylmethionine). The apparent K_m for putrescine was 20 μM. 1,3-diaminopropane, 1,5-diaminopentane and spermidine were weaker substrates with maximal rates at 37 °C of 24%, 4.4% and 4.6%,

respectively, of that of putrescine. Many thermophiles, including *T. maritima*[14], contain polyamines not found in mammals, such as thermine (symnorspermine) and caldine (symnorspermidine). By using 1,3-diaminopropane as substrate, TmPAPT may well be able to produce a significant amount of caldine.

TmPAPT was strongly inactivated by AdoDATO, a compound designed by Coward[2,15] to be a multisubstrate adduct inhibitor of PAPTs. The IC_{50} value was 0.2 μM, which compares well with values of 0.1–0.4 μM under similar assay conditions for other PAPTs[2,15]. Spermidine synthesis by TmPAPT had an optimal pH of 7.5 and was greatly increased at higher temperatures, with the k_{cat} value increasing from 0.08 s^{-1} at 37 °C to 3.3 s^{-1} at 90 °C.

Binding of AdoDATO

The difference Fourier electron density map for the apo and inhibitor-bound crystals allowed us to build AdoDATO molecules in subunits A, C and D of the tetramer (Fig 2*b*, 4*a*,*b*). In subunits A and D, the AdoDATO is almost completely buried within the protein, and its access to bulk solvent is blocked by loop 171−180; only part of the polyamine moiety is solvent exposed. The corresponding loop of subunit C makes numerous contacts with the symmetry-related molecule and adopts a drastically different conformation that is preserved in both structures. As a consequence, the AdoDATO bound to subunit C is partially disordered. All of the residues that interact with AdoDATO are conserved (Fig. 3), strongly supporting that the inhibitor–protein interaction observed in monomers A and D is functionally relevant. AdoMet donates a methyl group in many MTase reactions. Superposition of the TmPAPT catalytic core structure with those of AdoMet–MTase complexes revealed a very similar conformation and orientation of the adenosyl moiety. In TmPAPT, the adenosyl binding site is formed by the N-termini and the following loops of β-strands 7, 8 and 10. The loop between β3 and β4 also contributes to ribose binding. The carbon of the aminopropyl moiety linked to the sulfur of AdoDATO is oriented approximately in the same direction as the target methyl group of AdoMet in MTases. This orientation positions the target group of the aminopropyl moiety toward the putrescine binding cavity.

The AdoDATO aminopropyl moiety is in a similar orientation to the analogous part of AdoMet in MTases. However, the binding cavity in TmPAPT is narrower than the analogous cavity in MTases and cannot accommodate the carboxyl group of AdoMet, which is predicted to undergo a steric and electrostatic clash with the side chain of Asp 101. Asp 101 is conserved in PAPT and SAPT (data not shown) but not in methyltransferases such as putrescine N-methyltransferase (PNMT) (Fig. 3), which uses AdoMet as a cofactor to transfer a methyl group to putrescine to form N-methylputrescine and has very high sequence similarity to PAPT. The only substitutions of conserved residues in PAPT occur at or near the aminopropyl binding cavity, including substitution of Asp 101 by Ile, and likely contribute to the formation of a PNMT cavity suitable for the carboxyl group of AdoMet.

The polyamine moiety of AdoDATO is oriented toward a long, deep cleft between the N- and C-terminal domains formed by residues from loop β5–β6, β6, αA, loop β10–αE, loop β11–αF, β12 and loop β12–β13. The surface of the cavity is hydrophobic in the central region with negative charge distribution at both ends, which should anchor the amino groups of putrescine.

The length of this partially hydrophobic polyamine-binding cavity may be a key feature for selecting the polyamine with the appropriate number of CH_2 modules. The reduction in reaction rate with either 1,3-diaminopropane or 1,5-diaminopentane is presumably caused either by extra flexibility of the molecule inside the cavity or by the variations in distance between terminal amino groups, which would prevent precise positioning of the substrate for the reaction. To explain small residual activity with the longer polyamine, spermidine, we predict

that the 'putrescine-like' moiety can still fit the binding site, whereas the extra aminopropyl group would extend out into solvent.

'Gatekeeping' loop

The structures of the free and bound TmPAPT reveal a significant conformational change in the 171−180 loop upon binding of AdoDATO (Fig 2*a*, Fig 4*b*). In subunits A and D, the loop that becomes ordered only in the AdoDATO complex completely envelops the AdoDATO moiety and would also be predicted to cover the substrate and cofactor or their products. In contrast, crystal packing caused the loop to flip out of the substrate binding site of subunit C, leaving a large part of AdoDATO solvent exposed. Therefore, the 171–180 loop is effectively a gatekeeper to and from the active site.

The TmPAPT enzyme has four times as much spermine synthase activity (4.6%) as the other PAPTs (1%). The 'gatekeeping' loop of TmPAPT lacks one Pro and has an extra Gly residue compared to other PAPTs. Therefore, the TmPAPT loop may be more flexible, possibly accommodating longer substrates more efficiently.

Proposed catalytic mechanism of PAPT

The PAPT-catalyzed formation of spermidine from putrescine is suggested to occur by a single-displacement mechanism, with inversion of the configuration of the methylene carbon undergoing nucleophilic attack by putrescine[16]. In this mechanism, the interaction of PAPT with the amino group of putrescine would reduce the protonation and facilitate the electron transfer. Analysis of the structure points to Asp 170, which is conserved in all PAPT, PNMT and SAPT enzymes, as the most likely candidate to deprotonate the attacking amino group of putrescine. The corresponding residue in MTases is an Asp in the α- and β-classes of DNA amino-MTases and Asn in the γ-class[12], and was proposed to be a hydrogen bond acceptor for the target amino group.

In the AdoMet-dependent MTases, the main chain carbonyl group of the following Pro residue is also implicated in catalysis[17]. This group superimposes perfectly with the corresponding carbonyl of Ser 171 of TmPAPT. Tyr 76 is on the opposite side of the catalytic cavity with the OH group pointing towards C_{11}. It is also invariant in the PAPT, SAPT and PNMT enzymes. Thus, the current structure points to Asp 170 as the best candidate for deprotonation of putrescine, whereas Ser 171 and Tyr 76 may be important for binding and proper orientation of putrescine.

Methods

Reagents

The dcAdoMet and AdoDATO preparations used were generously provided by A. Shirahata (Josai University, Japan) and J.K. Coward (University of Michigan, Ann Arbor), respectively. [^{35}S]dcAdoMet was synthesized enzymatically, as described[18].

Sample preparation and crystallization

TmPAPT was subcloned, the recombinant protein expressed and purified, and initial crystal trials were performed as previously described[19]. Diffraction quality crystals were obtained from hanging drop vapor diffusion conditions containing 2 μl protein plus 2 μl precipitant in 6% (w/v) PEG 4000 and 50 mM sodium acetate, pH 4.4, over 2–5 d at 21 °C. The crystals were flash-frozen with the crystallization buffer plus 20% (v/v) glycerol. Native TmPAPT (10 mg ml^{-1}) was incubated with 0.3 mM AdoDATO for 10 min at 37 °C in 10 mM HEPES, pH 7.5, and 0.5 M NaCl prior to crystallization.

Enzyme assay

Aminopropyltransferase activity was measured by following the production of [^{35}S]MTA from [^{35}S]dcAdoMet in the presence of either putrescine or spermidine as an aminopropyl acceptor[18]. The standard assay medium contained 100 mM sodium phosphate buffer, pH 7.5, 10 μM dcAdoMet and 0.25 mM putrescine. Reactions were run for 30 min with an amount of enzyme that gave a linear MTA production rate at 37 °C and for 2 min at higher temperatures. The formation of spermidine from putrescine and unlabeled dcAdoMet was measured after separating the products of the reaction by ion-pair reversed-phase HPLC and post-column derivatization with O-phthaldehyde.

Molecular weight determination

HPLC size-exclusion chromatography was performed on a Superose-12 HR column (10 × 300 mm^2) pre-equilibrated with 10 mM HEPES, pH 7.5, and 0.5 M NaCl. The column was calibrated with cytochrome c (12.4 kDa), carbonic anhydrase (29 kDa), bovine serum albumin (66 kDa), alcohol dehydrogenase (150 kDa), β-amylase (200 kDa) and Blue Dextran (2,000 kDa). Protein samples of 25 μl PAPT at 2 mg ml^{-1} concentration or premixed with standard proteins were centrifuged at 14,000 rpm for 10 min before injection into the column through a 20 μl injection loop. Filtration was carried out at 20 °C at a flow rate of 1 ml min^{-1}. The eluted proteins were detected by measuring the absorbance at 280 nm.

Data collection, phasing, structure determination and refinement

The TmPAPT crystallized in space group $P2_12_12$ with unit cell parameters a = 132.4 Å, b = 197.8 Å and c = 52.6 Å, and contains four subunits (131 kDa) in the asymmetric unit (V_m = 2.7). All data were collected at beamline 19ID of the Structural Biology Center at the APS, ANL. Thirty Se peaks were found using Shake-and-Bake[20]. Phases were calculated with SOLVE[21] at 2.4 Å resolution and extended to 1.6 Å using DM[22], and 1,100 residues were built automatically using ARP/wARP[23]. An additional 40 residues were built manually using O[24].

The crystals of the TmPAPT–AdoDATO complex have almost identical unit cell parameters to those of TmPAPT, and the coordinates of the native protein were used for initial refinement of TmPAPT–AdoDATO structure. The AdoDATO molecules were built using HIC-Up (Hetero-compound information center, Uppsala) and O[24]. Both structures were refined with CNS v1.0 (ref. [25]) and without any NCS restrictions. Statistics of data collection and refinement are shown in Table 1.

Coordinates

Atomic coordinates and structure factors have been deposited into the Protein Data (accession codes 1INL for TmPAPT and 1JQ3 for the complex with AdoDATO).

Acknowledgments

We wish to thank all members of the SBC at ANL for their help in conducting experiments and L. Keller for help in preparation of this manuscript. This work was supported by the National Institutes of Health; the U.S. Department of Energy, Office of Biological and Environmental Research; the Ontario Research and Development Challenge Fund; and National Institutes of Health. A.M.E. and C.H.A. are CIHR Investigators. The submitted manuscript has been created by the University of Chicago as Operator of Argonne National Laboratory (‘Argonne’) under contract with the U.S. Department of Energy. The U.S. Government retains for itself, and others acting on its behalf, a paid-up, nonexclusive, irrevocable worldwide license in said article to reproduce, prepare derivative works, distribute copies to the public, and perform publicly and display publicly, by or on behalf of the Government.

References

1. Pegg AE. Biochem J 1986;234:249–262. [PubMed: 3087344]

2. Pegg AE, Poulin R, Coward JK. Int. J. Biochem. Cell Biol 1995;27:425–442. [PubMed: 7641073]
3. Lakanen JR, Pegg AE, Coward JK. J. Med. Chem 1995;38:2714–2727. [PubMed: 7629810]
4. Tang KC, Pegg AE, Coward JK. Biochem. Biophys. Res. Commun 1980;96:1371–1377. [PubMed: 7437076]
5. Rossmann, MG.; Liljas, A.; Branden, C-I.; Banaszak, LK. Oxidation-reduction. Boyer, PD., editor. New York: Academic Press; 1975. p. 61-102.
6. Fauman, EB.; Blumenthal, RM.; Cheng, X. S-Adenosylmethionine-dependent methyltransferases. Cheng, X.; Blumenthal, RM., editors. Singapore: World Scientific Publishing; 1999. p. 1-38.
7. Holm L, Sander C. Nucleic Acids Res 1996;24:206–209. [PubMed: 8594580]
8. Vidgren J, Svensson LA, Liljas A. Nature 1994;368:354–358. [PubMed: 8127373]
9. Fu Z, et al. Biochemistry 1996;35:11985–11993. [PubMed: 8810903]
10. Schluckebier G, Kozak M, Bleimling N, Weinhold E, Saenger W. J. Mol. Biol 1997;265:56–67. [PubMed: 8995524]
11. Hofmann K, Bucher P, Falquet L, Bairoch A. Nucleic Acids Res 1999;27:215–219. [PubMed: 9847184]
12. Malone T, Blumenthal RM, Cheng X. J. Mol. Biol 1995;253:618–632. [PubMed: 7473738]
13. Salminen T, et al. Protein Sci 1996;5:1014–1025. [PubMed: 8762133]
14. Hamana K, et al. Microbios 1998;94:7–21.
15. Shirahata A, Takahashi N, Beppu T, Hosoda H, Samejima K. Biochem. Pharmacol 1993;45:1897–1903. [PubMed: 8494549]
16. Orr GJ, et al. J. Am. Chem. Soc 1988;110:5791–5799.
17. Scavetta RD, et al. Nucleic Acids Res 2000;28:3950–3961. [PubMed: 11024175]
18. Wiest, L.; Pegg, AE. Methods in molecular biology. Morgan, DML., editor. Vol. Vol. 79. Totowa, New Jersey: Humana Press; 1997. p. 51-58.
19. Zhang R-G, et al. Structure 2001;9:1095–1106. [PubMed: 11709173]
20. Hauptman HA. Methods Enzymol 1997;277:3–13. [PubMed: 9379923]
21. Terwilliger TC, Berendzen J. Acta Crystallogr. D 1999;55:849–861. [PubMed: 10089316]
22. Cowtan K, Main P. Acta Crystallogr. D 1998;54:487–493. [PubMed: 9761844]
23. Perrakis A, Morris R, Lamzin VS. Nature Struct. Biol 1999;6:458–463. [PubMed: 10331874]
24. Jones TA, Zou JY, Cowan SW. Kjeldgaard. Acta Crystallogr. A 1991;47:110–119.
25. Brünger AT, et al. Acta Crystallogr. D 1998;54:905–921. [PubMed: 9757107]
26. Abagyan RA, Totrov MM, Kuznetsov DN. J. Comp. Chem 1994;15:488–506.
27. Thompson JD, Higgins DG, Gibson TJ. Nucleic Acids Res 1994;22:4673–4680. [PubMed: 7984417]
28. Gouet P, Courcelle E, Stuart DI, Metoz F. Bioinformatics 1999;15:305–308. [PubMed: 10320398]
29. Wallace AC, Laskowski RA, Thornton JM. Protein Eng 1995;8:127–134. [PubMed: 7630882]
30. Laskowski RA, MacArthur MW, Moss DS, Thornton JM. J. App. Crystallogr 1993;26:283–291.

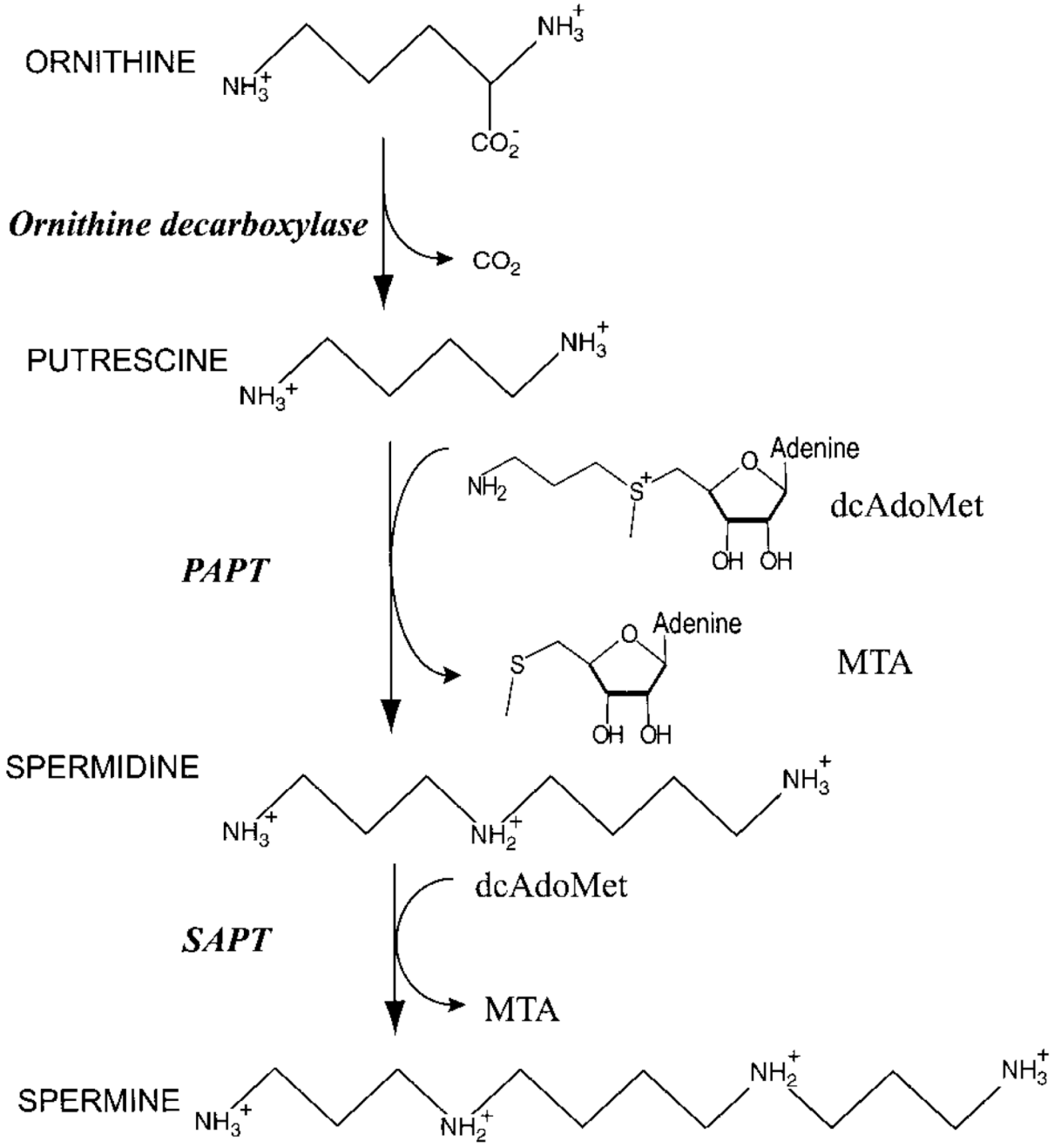

Fig. 1.
General pathway for the biosynthesis of putrescine, spermidine and spermine.

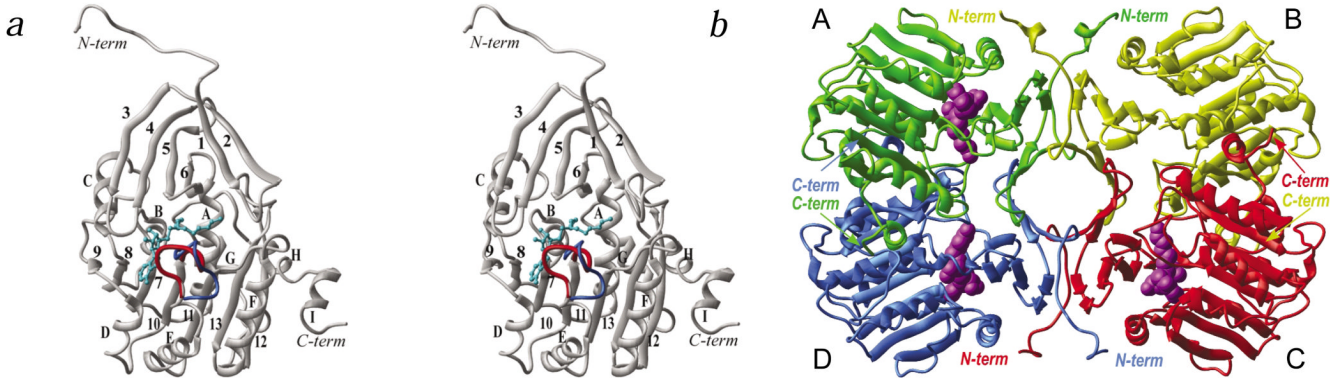

Fig. 2.

Overall structure of TmPAPT monomer and architecture of the tetramer. ***a***, Stereo view of a ribbon diagram representation of TmPAPT subunit D. The α-helixes are lettered, and β-strands are numbered. AdoDATO is shown in ball-and-stick representation in cyan. The 'gatekeeping' loop is shown in red. The conformation of the analogous loop in subunit C upon superposition with subunit D is shown in blue. All structural figures, except Fig. 4*a*, are made with the ICM[26]. ***b***, Architecture of the TmPAPT tetramer. Ribbon diagrams of subunits A, B, C and D are shown in green, yellow, red and blue, respectively. AdoDATO is shown in CPK representation in magenta. The absence of AdoDATO in subunit B can be explained by the presence of additional electron density near the substrate binding site in both structures, which most likely corresponds to a partially ordered PEG molecule important for crystal packing and preventing AdoDATO from binding to subunit B.

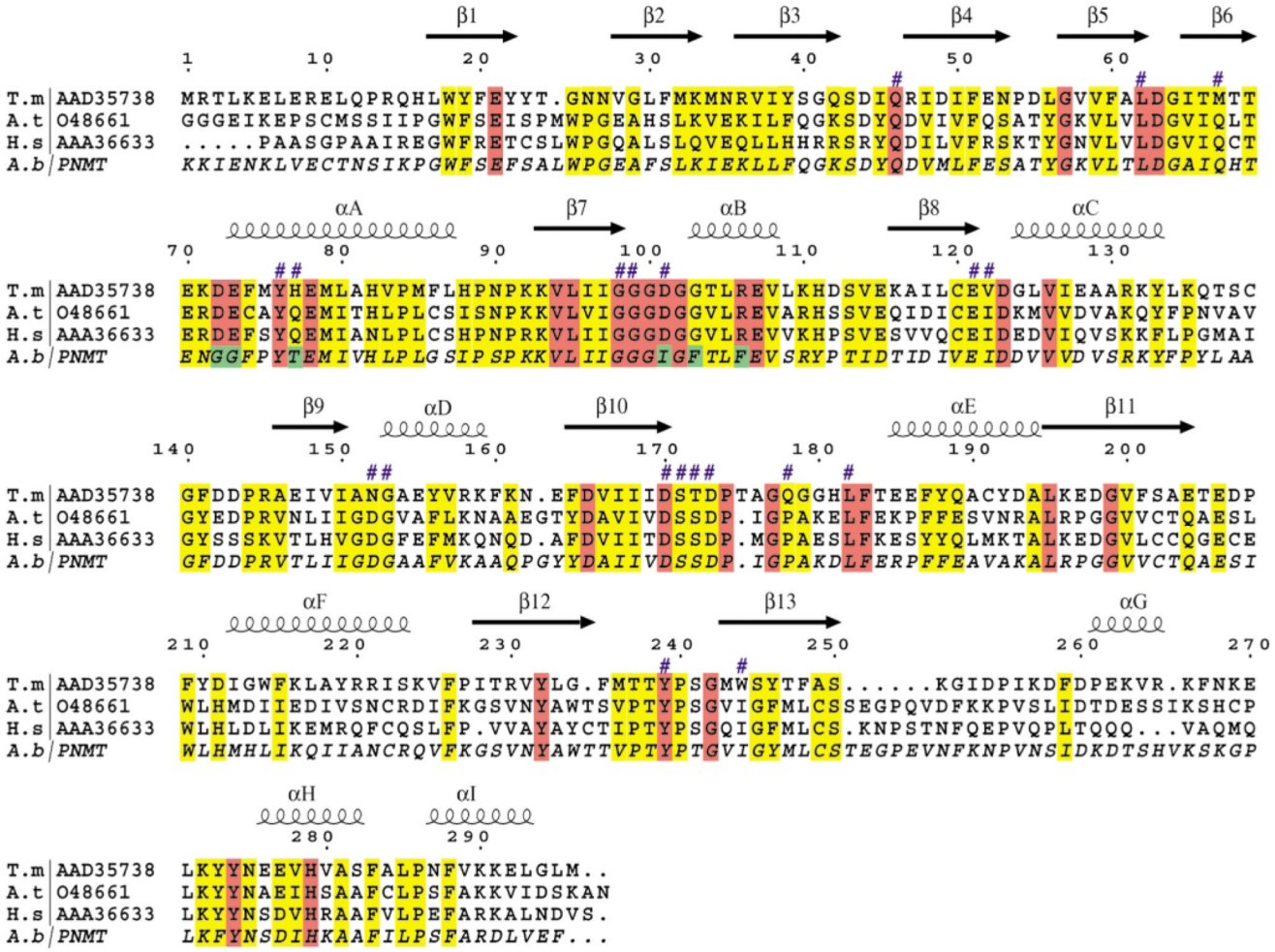

Fig. 3.

Sequence alignment of TmPAPT with plant and human PAPTs and with PNMT. Color coding of conserved residues by yellow boxes and invariant residues by red boxes is based on alignment of 19 PAPT sequences from various species (data not shown). Out of the >70 putative aminopropyltransferase sequences in the database, only sequences that have been shown to encode a PAPT by enzymatic assay of the expressed protein or by genetic deletion analysis and those derived from species known to contain only spermidine as the higher polyamine were selected for multiple alignment. Accession numbers are shown on the left. Secondary structure elements of TmPAPT are shown on the top. Numbering is shown for the TmPAPT sequence only. The blue number signs are shown on the top of TmPAPT residues interacting with AdoDATO. The bottom sequence is PNMT from *Atropa belladona* (BAA82264). Residues of PNMT that deviate from conserved residues of PAPT are shown in green boxes. Sequence alignment was generated by CLUSTALW[27] and displayed with ESPrit[28].

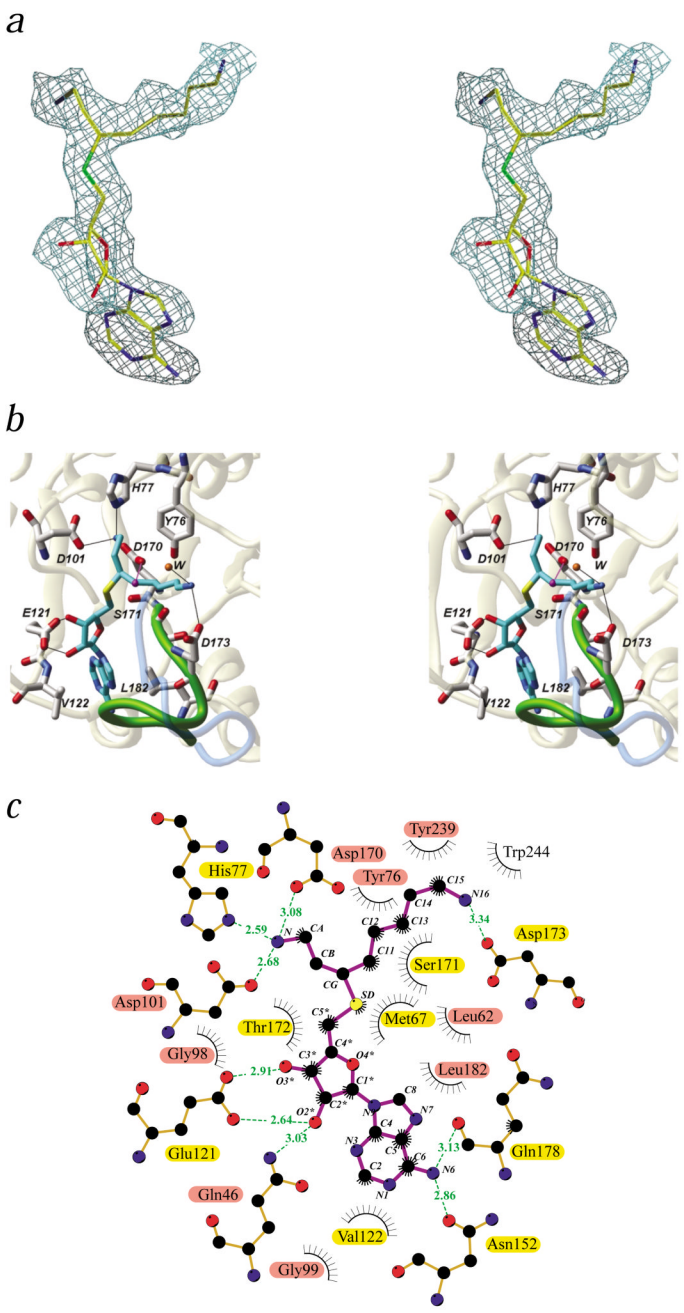

Fig. 4.

Interaction of AdoDATO with TmPAPT. ***a***, A stereo view of $F_o - F_c$ electron density map produced by omitting the AdoDATO from the model during simulated annealing refinement and map calculation, and contoured at 2.0 σ level around AdoDATO bound to subunit D (generated with O[24]). ***b***, Close-up stereo view of substrate binding site. The view is shown from the N-terminal domain toward the C-terminal domain. AdoDATO and selected residues involved in inhibitor binding are shown in stick representation. Nitrogens, oxygens and sulfurs are shown in blue, red and yellow, respectively. Carbons of TmPAPT residues are shown in gray, and carbons of AdoDATO are shown in cyan. The water molecule is shown as an orange sphere. Hydrogen bonds are shown by thin black lines. The C-terminal domain is shown in

light yellow transparent ribbon representation. The gatekeeping loop is shown by green worm representation and the corresponding loop of subunit C by transparent blue worm representation. The C11 group of AdoDATO corresponding to attacking amino group of putrescine is highlighted by magenta. The proposed hydrogen bond involved in deprotonation of the corresponding amino group of putrescine is shown by a magenta line. ***c***, Schematic LIGPLOT[29] diagram of the interactions between AdoDATO (bonds shown in violet) and TmPAPT. Protein side chains that form hydrogen bonds with AdoDATO are shown with bonds in orange. Hydrogen bonds are drawn as dashed lines, and the donor-acceptor distances are given. Residues involved in hydrophobic interactions are shown with arcs. Residue names and numbers are highlighted by colors corresponding to colors on structural alignment picture (Fig. 3).

Table 1

Data collection and refinement statistics

Crystal	**Native**	**Peak**	**SeMet Inflection**	**Low remote**	**AdoDATO**
Wavelength (Å)	0.97934	0.97925	0.97938	0.99187	0.97948
Resolution (Å)	50–1.5	50–2.3	50–2.3	50–2.3	50–1.75
R_{merge} (%)[1]	8.6 (24.2)	8.4 (34.5)	9.5 (47.2)	8.7 (50.6)	7.6 (55.6)
Completeness (%)[1]	95.2 (81.4)	99.3 (98.9)	99.6 (99.4)	99.1 (98.8)	91.3 (72.5)
I / σ (I)[2]	4	3.7	2.5	1.8	1.9
Refinement					
Crystal	Native		AdoDATO complex		
Resolution (Å)	50–1.5		50–1.8		
Number atoms					
Protein non-H	9,344		9,484		
Substrate non-H	0		87		
Water molecules	1200		743		
Number of reflections					
Working set	197,073		112,302		
Test set (5%)	10,174		5,940		
R-factor (%)[1]	19.9 (22.8)		19.6 (25.1)		
R_{free} (%)[1]	21.3 (25.0)		22.9 (29.0)		
R.m.s. deviations					
Bonds (Å)	0.009		0.009		
Angles (°)	1.4		1.4		
B-factors (Å^2)					
Overall	18		22		
Ligands[2]	–		31, 44, 29		
Water	33		32		
Ramachandran plot (%)[3]					
Most favored	90.1		88.9		
Allowed	8.6		9.8		
Generously allowed	1.3		1.3		
Disallowed	0.0		0.0		

[1] Values for highest resolution shell (1.5–1.55 Å for native and 1.8–1.91 Å for AdoDATO complex) are shown in parentheses.

[2] Three values are shown for AdoDATO molecules bound to chains A, C and D, respectively.

[3] Ramachandran plot parameters were calculated by program PROCHECK[30].